Chemical and structural changes of calcium ion exchange silica pigment in 0.5M NaCl and 0.5M Na_2SO_4 solutions

N. Granizo[1,*], M.I. Martín[1], F.A. López, J.M. Vega, D. de la Fuente and M. Morcillo
National Centre for Metallurgical Research (CENIM/CSIC), Avda. Gregorio del Amo, 8, 28040 Madrid, Spain

Cambios químicos y estructurales del pigmento sílice/calcio en soluciones de NaCl y Na_2SO_4 0.5M

Canvis químics i estructurals del pigment sílice/calci en solucions de NaCl i Na_2SO_4 0,5M

Recibido: 25 de octubre de 2011; revisado: 13 de febrero de 2012; aceptado: 14 de febrero de 2012

RESUMEN

Este trabajo estudia la viabilidad de un pigmento anticorrosivo medioambientalmente aceptable para la sustitución de los pigmentos de Cr (VI), caracterizando el pigmento de partida y los productos obtenidos después de su interacción con soluciones de iones agresivos desde el punto de vista de la corrosión (Cl^- and SO_4^{2-}). Las técnicas utilizadas para ello fueron difracción de rayos X (DRX), calorimetría (DTA-TG), espectroscopía de IR con transformada de Fourier (FTIR) y microscopía electrónica de barrido/espectrometría de energías dispersivas (SEM-EDAX). Se estudió la capacidad de intercambio iónico del pigmento y se analizaron las soluciones obtenidas después de la interacción pigmento-solución. Los resultados obtenidos muestran que tiene lugar unas serie de transformaciones físico-químicas en el pigmento cuando interacciona con los iones Cl^- y SO_4^{2-}, en algunos casos acompañado de la aparición de nuevas fases cristalinas, principalmente silicatos de calcio y sodio y sulfato de sodio. Los análisis de las soluciones obtenidas después de la interacción muestran un incremento en el contenido de calcio según aumenta la fuerza iónica del medio. Estos resultados sugieren que el mecanismo por el cual el pigmento actúa no solo está basado en reacciones de intercambio iónico, sino que también existen modificaciones estructurales, la propia solubilidad del pigmento en el medio y consecuentemente reacciones de (co)precipitación que dan lugar a compuestos insolubles en el medio agresivo estudiado.

Palabras clave: Sílice/calcio, pigmento, intercambio iónico, anticorrosivo, XRD, SEM-EDAX, FTIR, DTA- TG

SUMMARY

This paper studies the suitability of an environmentally-friendly anticorrosive pigment (Si/Ca) to replace Cr(VI) pigments, characterising the initial pigment and the products obtained after interaction with aqueous solutions containing aggressive ions from a corrosion viewpoint (Cl^- and SO_4^{2-}). X-ray diffraction (XRD), calorimetry (DTA-TG), Fourier transform IR spectroscopy (FTIR) and scanning electron microscopy (SEM-EDAX) techniques are used. The ion exchange capacity of the pigment is studied and the solutions obtained after the pigment-solution interaction are analysed. The results obtained show that a series of physical/chemical transformations take place in the pigment on interaction with the Cl^- and SO_4^{2-} solutions, in some cases accompanied by the appearance of new crystalline phases, mainly calcium and sodium silicates and calcium sulphate. Analysis of the solutions obtained after interaction shows a rise in the calcium content as the ionic force of the medium increases. These results suggest that the mechanism by which the pigment acts is not only based on ion exchange reactions but also on a structural modification of the pigment itself and consequently on (co) precipitation reactions that form insoluble compounds in the studied aggressive media.

Keywords: Silica/calcium, pigment, ion-exchange, anti-corrosion, XRD, SEM-EDAX, FTIR, DTA-TG

RESUM

Aquest treball estudia la viabilitat d'un pigment anticorrosiu mediambientalment acceptable per a la substitució dels pigments de Cr (VI), caracteritzant el pigment de partida i els productes obtinguts després de la seva interacció amb solucions de ions agressius des del punt de vista de la corrosió (Cl^- i SO_4^{2-}). Les tècniques utilitzades van ser difracció de raigs X (DRX), calorimetria (DTA-TG), espectroscòpia d'IR amb transformada de Fourier (FTIR) i microscòpia electrònica de rastreig / espectrometria d'energies dispersives (SEM-EDAX). Es va estudiar la capacitat d'intercanvi iònic del pigment i es van analitzar les solucions obtingudes després de la interacció pigment-solució. Els resultats obtinguts mostren que tenen lloc

*Corresponding author: Department of Materials Synthesis, Characterization and Stability, Eduardo Torroja Institute for Construction Science (IETCC-CSIC). Serrano Galvache, 4, 28033 Madrid, Spain.
Tel. +34 91 302 04 40; fax: +34 91 302 07 00 ; noeliag@ietcc.csic.es [1] At present, Eduardo Torroja Institute for Construction Science (IETCC/CSIC), Serrano Galvache, 4, 28033 Madrid, Spain.

unes sèries de transformacions físico-químiques en el pigment quan interacciona amb els ions (Cl^- i SO_4^{2-}), en alguns casos acompanyat de l'aparició de noves fases cristal·lines, principalment silicats de calci i sodi i sulfat de sodi. Les anàlisis de les solucions obtingudes després de la interacció mostren un increment en el contingut de calci quan augmenta la força iònica del medi. Aquests resultats suggereixen que el mecanisme pel qual el pigment actua no només està basat en reaccions d'intercanvi iònic, sinó que també hi ha modificacions estructurals, la pròpia solubilitat del pigment en el medi i conseqüentment reaccions de (co)precipitació que donen lloc a compostos insolubles en el medi agressiu estudiat.Paraules clau: Sílice / calci, pigment, intercanvi iònic, anticorrosiu, XRD, SEM-EDAX, FTIR, DTA-TG

1. INTRODUCTION

In recent decades efforts have increasingly focused on the search for environmentally friendly alternatives to replace Cr(VI) pigments due to their toxicity to human health [1] and the environment [2]. As a result, more efficient and versatile pigments have been developed [3-4].

Calcium ion exchange silica (silica/calcium (Si/Ca)), marketed in the 1980's by the company W. R. Grace Davison under the brand name Shieldex®, has proven to be a valid environmentally friendly alternative to Cr(VI) pigments. The chemical nature of this product and its physical and structural properties, like its high specific surface area (around 60 $m^2 \cdot g^{-1}$), allow it to act either by adsorption/desorption reactions or ion exchange reactions [5].

Since that time, research on silica/calcium has grown exponentially, seeking to determine its anticorrosive effectiveness and to settle controversies regarding its action mechanisms, exchange capacity, etc. Most papers attribute an ion exchange mechanism, i.e. the retention and immobilisation of aggressive species (H^+, Cl^-, etc.) from the medium and the release of species that inhibit metallic corrosion and/or form protective layers on the metallic surface, Ca^{2+} and polysilicate ions (Figure 1) [6-12]. However, some studies suggest that anticorrosive protection may be due more to a passivation process of the steel as a consequence of the high pH of the pigment's aqueous solution (pH ~ 9) and the deposition of a siliceous film on the steel surface (iron silicate) rather than an ion exchange capacity between Ca^{2+} and aggressive ions [13-14].

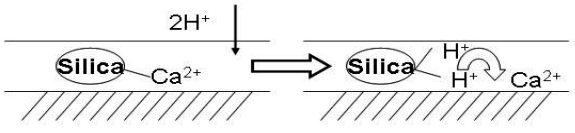

Figure 1. *Scheme of mechanism by which aggressive ions (H^+) are retained and inhibitor (Ca^{2+}) is released from the silicon/calcium cation exchange pigment.*

In previous studies the authors have assessed the inhibiting efficiency of this pigment incorporated in organic coatings applied on steel [15] and aluminium [16] surfaces, and the metallic surfaces and the solutions obtained after the pigment/electrolyte interaction have been analysed [17].

The aim of this work is to contribute to the better understanding of the mechanism by which the pigment acts and to compare the results obtained with those reported in the literature. Hitherto, studies have been based on identifying any film formed on the metallic surface and analysing the pigment solution after its interaction with the aggressive ions in the environment, but not on characterising the solids obtained after the pigment/electrolyte interaction, which is main objective of the present work. The aqueous solutions obtained after the pigment/electrolyte interaction are also analysed, comparing the data yielded with the Si/Ca pigment and a traditional Cr(VI) pigment. The results obtained in the relation solid/liquid study allow interesting conclusions to be drawn about the anticorrosive mechanism of the Si/Ca pigment.

2. EXPERIMENTAL

The silica/calcium (Si/Ca) anticorrosive pigment used was a commercial product (AC5 W.R. GRACE Davison) with a maximum particle size of 5 µm.

The Cr(VI) anticorrosive pigment used was a commercial zinc chromate (Nubiola Inorganic Pigments) with a particle size of no more than 30 µm.

Aqueous suspensions of the Si/Ca pigment were prepared in 0.5M NaCl and 0.5M Na_2SO_4 solutions with a concentration of 10 $g.L^{-1}$ to study ion exchange properties and characterise the solids resulting from the pigment/electrolyte interaction. The suspensions were kept in continuous stirring for 24 h to reach equilibrium and then separated by centrifugation (9000 rpm for 5 minutes) and filtered with a 2.5 µm filter. The aqueous solutions were collected for analysis and the resulting solids were dried at room temperature and pulverised for their subsequent study.

The same experimental procedure used with the Si/Ca pigment, keeping the same solution concentration (10 $g \cdot L^{-1}$), was also applied for comparative purposes with the Cr(VI) zinc chromate pigment

2.1. Characterisation of solids

The chemical composition was determined by micro-X-ray fluorescence (XRF) using a Brucker S8 Tiger unit with a wolfram tube, a LiF analyser crystal and a 4 Kw generator.

The zeta potential of the pigment was determined at ambient temperature using a Zeta-Meter 3.0+ unit. Pigment suspensions with a concentration of $7 \cdot 10^{-2}$ $g \cdot L^{-1}$ were prepared using a 10^{-2} M KCl solution. All the suspensions were broken up in ultrasound for 2 minutes and kept in continuous stirring for 24 h prior to performing the measurement. The variation in zeta potential with pH was also studied using an automatic titrator connected to the potential meter.

Physical/chemical characterisation was performed by Fourier transform infrared spectrometry (FTIR), thermogravimetric analysis (DTA-TG), X-ray diffraction (XRD) and scanning electron microscopy - energy dispersive X-ray spectroscopy (SEM-EDAX).

Infrared spectra were obtained using a Nicolet Magna-IR™ 550 spectrometer. Spectra were acquired in the 400-4000 cm^{-1} range. Samples were prepared by mixing the solids in powder with ICs at a weight ratio of 15:85.

DTA-TG was carried out simultaneously using a SETARAM DTA-TG Setsys Evolution 1750 thermobalance in a helium atmosphere (20 $mL \cdot min^{-1}$). Previously homogenised samples of around 20 mg were heated in alumina crucibles. A record was made of the weight losses experienced in

the 25ºC-800ºC temperature range. A heating rate of 20ºC·min^{-1} was used in all cases.

The crystalline structure of the initial pigment and the pigment/electrolyte interaction products was determined by XRD using a Philips model X'Pert diffractometer with CuKα radiation (λ= 0.1541 nm) and a Ni filter. Data was collected in the range between 10º and 100º in 2θ scale at a rate of 0.1º·min^{-1}.

Morphological and structural characteristics of Si/Ca were obtained by SEM with a JEOL JSM 6500F field emission SEM unit equipped with secondary and backscattered electron detectors and an EDAX brand EDS detector. Samples were prepared by embedding in resin, surface polishing with diamond paste, and coating with graphite.

2.2. Ion exchange capacity

The cation content in the aqueous extract obtained after the pigment/electrolyte interaction was determined by atomic absorption spectrometry (AAS) using a Varian FS-220 spectrophotometer. This equipment is provided with a laminar flow burner for air-acetylene flame, for the analysis of Zn, and nitrous oxide-acetylene flame for the analysis of Ca and Cr ions. Before starting to analyse the samples a calibration curve was created for each element, entering previously prepared standards of a known concentration of each element. All the samples were performed in duplicate.

To evaluate the effect of pH on ion exchange process, 0.1 M H_2SO_4, 0.1 M HCl and 0.1 M NaOH solutions were added to the study solutions (0.5M Na_2SO_4 and 0.5M NaCl) to adjust the pH to 4.6, 6.2 and 10, following the same procedure described above. As blank solution and as a measure of the solubility of the different pigments, the study was carried out with deionised water and at the different pH values.

Table 1*.Chemical composition of Si/Ca pigment and the solids obtained after its exposure to different media.*

		Chemical composition (% weight)							
Sample	electrolyte pH	Ca	Si	O	Na	H	S	Cl	Si/Ca
Si/Ca	-	5.33	36.67	56.29	0	1.5	0	0	6.9
Si/Ca/0.5M Na_2SO_4	4.60 7.10 10.00	2.60 2.67 3.45	25.56 27.39 30.80	63.72 62.72 59.78	3.1 2.98 2.42	3.9 3.6 2.7	1.01 0.67 0.85	0 0 0	9.8 10.2 8.9
Si/Ca/0.5M NaCl	4.60 6.50 10.00	3.10 3.78 3.00	24.45 27.05 22.29	65.09 62.76 66.87	1.95 1.63 1.76	4.4 3.8 5.0	0 0 0	0.95 1.01 1.07	7.9 7.2 7.4
Si/Ca/H_2O	4.60 7.10 10.00	3.64 4.97 3.46	25.55 34.23 22.69	66.31 58.58 68.63	0 0 0	4.5 2.2 5.2	0 0 0	0 0 0	7.1 6.9 6.6

3. RESULTS AND DISCUSSION

3.1. Characterisation of Si/Ca pigment

The Si/Ca pigment consists fundamentally of Si, O and Ca, with a 5.3 wt% content of the latter (Table 1). The Si/Ca ratio is equal to 6.9/1, a value very close to that obtained by *Armstrong* (7.5/1) [11]. The total mass loss in the 50ºC to 800ºC temperature interval is 13.61 wt%, which is equivalent to 4.6 water molecules, very close to the value found by *Armstrong* and *Deflorian* [11,9]. Therefore, the formula of the characterised commercial pigment could present the formula: CaO (7)·SiO_2 (4.6)·H_2O

The Si/Ca pigment shows an amorphous crystalline structure with an intense, broad and poorly defined peak at 25º (2θ) (Figure 2). The morphology of the Si/Ca particles, as depicted in Figure 3, shows an irregular appearance with different grain sizes (3.6-5 μm). The Si/Ca particles are seen to have well defined edges with rounded sides.

FTIR characterisation of the Si/Ca pigment (Figure 4) reveals the existence of two types of vibrational bands, those corresponding to vibration modes of the O-H bond and those related with the Si-O and Si-O-Si bonds.

The bands corresponding to vibration mode of the O-H bond correspond to humidity, absorbed water and, to a lesser extent, the possible presence of hydroxides in the sample. These bands, of low intensity, appear at the wavelengths of 3517 cm^{-1}, fundamental stretch vibration of the O-H bond, and 1647 cm^{-1}, assigned to angular deformation of the O-H bond in water molecules [18-22].

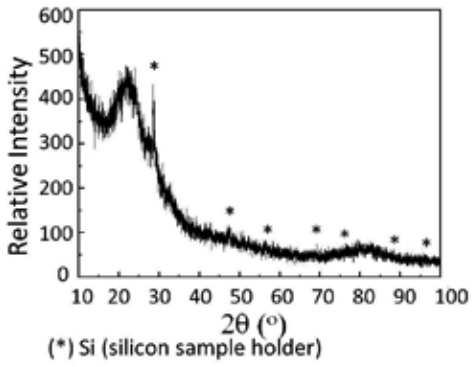

Figure 2*. X-ray diffractogram of Si/Ca pigment.*

The bands related with vibration mode of the Si-O bond [18-21, 23, 24] are bands of greater intensity. The band at 1087 cm^{-1}, ν_3 (Si-O), whose width goes from 950 to 1300 cm^{-1}, is composed of two shoulders, the left shoulder centred at 950 cm^{-1} is assigned to vibration of Si-OH (silanols), and the shoulder situated on the right centred around 1150 cm^{-1} corresponding to asymmetric stretching movements of the bond Si-O-Si "asymmetrical stretch".

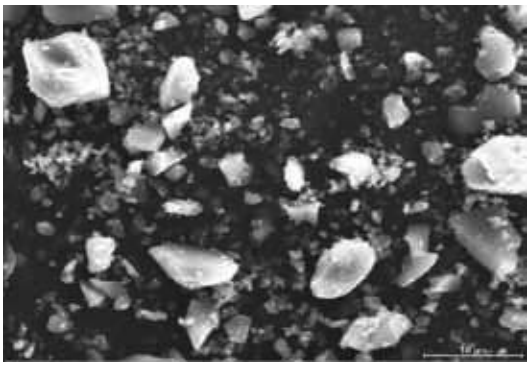

Figure 3. *Morphology of Si/Ca pigment particles observed by SEM.*

This band indicates the formation of a SiO_2 network and is highly characteristic in the identification of "silica gel" [20]. The bands at 798 and 466 cm^{-1} corresponds to vibrations modes of the Si-O-Si bond (ν4). These two bands are associated with angular deformations of the basic structure of SiO_2. The lowest vibration mode (at 466 cm^{-1}) is assigned to rocking motions, perpendicular to the Si–O–Si plane, and the bending movement out-of-plane to the vibration band at 798 cm^{-1}.

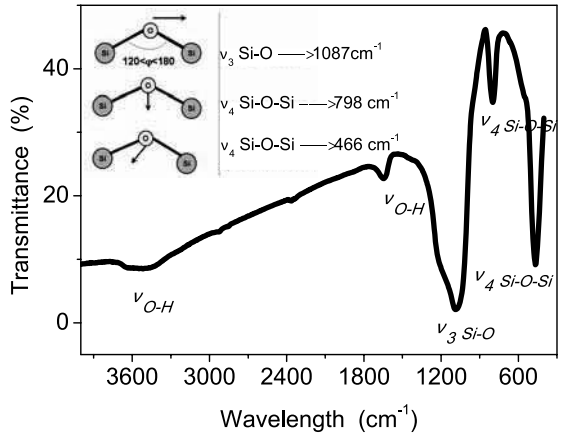

Figure 4. *FTIR spectrum of Si/Ca pigment.*

The incorporation of calcium in the siliceous matrix may be possible if the Ca-O-Si bond is formed, which according to the literature seems to present a vibration between 600 and 500 cm^{-1} [24-26]. The small amount of calcium in the solid makes it impossible to detect the vibration of the Ca-O-Si bond, which is masked by the vibration modes of greater intensity ν4 (Si-O-Si).

From the physical-chemical study it may be deduced that the pigment is constituted by an amorphous, colloidal inorganic matrix of silicon oxide upon whose surface some sites (hydroxyls) have been exchanged for calcium. The Si/Ca presents a high surface area (60 $m^2 \cdot g^{-1}$) [5], which makes it a solid upon which a large number of surface processes (adsorption/desorption, ion exchange, etc.) may take place.

Figure 5 shows the variation in the zeta potential of the Si/Ca pigment, constituted by hydroxyl groups across the surface of the solid, as a function of the pH. The results indicate that the pigment surface is negatively charged throughout the measured range, as a consequence of deprotonation of the hydroxyl groups on the surface. The negative surface charge is greater at alkaline pH values. These results clearly show a favourable exchange of Ca^{2+} ions throughout the pH range, but especially at alkaline pH values.

Table 2 shows the pH of the Si/Ca aqueous anticorrosive extracts prepared in 0.5M NaCl, Na_2SO_4 and deionised water. The pH values of the extracts, which are practically constant and close to 9, are not affected by variations in the medium pH, and ratify the buffer effect of the Si/Ca, i.e. its capacity to resist pH variations, which is directly related with the proportion of surface groups present on the solid. Thus it can be seen that pH variations in the medium are not sufficiently important to interact with all the surface groups present on the solid.

As with Si/Ca, the extracts prepared with zinc chromate in the different media show pH values that are independent of pH variations in the aggressive solution and close to neutrality (~6.7), as was to be expected, since only dissolution processes take place with this salt and so it does not present buffer properties.

Table 2. *Calcium and zinc content in aqueous anticorrosive extracts of Si/Ca and $ZnCrO_4$ pigments in different media.*

	Si/Ca			**$ZnCrO_4$**			
	electrolyte pH	extract pH	[Ca(II)], mg·g pigment^{-1}	electrolyte pH	extract pH	[Cr(VI)], mg·g pigment^{-1}	[Zn(II)], mg·g pigment^{-1}
H_2O	4.60	9.75	1.88	4.60	6.70	35.19	26.00
	7.10	9.70	1.83	7.20	6.70	34.50	23.25
	10.00	9.70	1.79	10.00	6.70	35.53	23.75
0.5M NaCl	4.60	9.40	10.00	4.60	6.60	57.50	60.50
	6.50	9.50	8.45	6.70	6.60	56.50	57.50
	10.00	9.40	7.55	10.00	6.60	56.50	44.00
0.5M Na_2SO_4	4.60	9.75	12.38	4.60	6.90	115.50	110.50
	7.10	9.75	12.63	6.30	6.90	117.00	113.00
	10.00	9.80	15.82	10.00	6.90	108.50	85.00

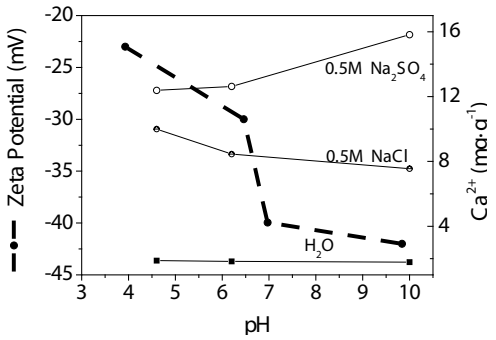

Figure 5. *Variation of zeta potential (mV) of Si/Ca pigment and cation exchange capacity (Ca^{2+}, $mg \cdot g^{-1}$) with the pH of different media.*

3.2. Ion exchange capacity of Si/Ca in 0.5M Na_2SO_4

The calcium content in the solution obtained after immersion of the Si/Ca pigment in 0.5M Na_2SO_4 (see Table 2) is considerably higher than in water (1.83 $mg \cdot g^{-1}$).

and Zn) anticorrosive extract shows much higher values in the latter case, following the same tendency with the 0.5M NaCl and blank solutions, thus corroborating the nature of the zinc chromate mentioned in foregoing paragraphs, without ion exchange properties and highly soluble. Furthermore, and as a characteristic of the soluble salts, the Cr and Zn content in the aqueous solution increases as the ionic force of the medium rises.

The exchange capacity increases as the pH of the solution rises, in concordance with the variation in the zeta potential of the pigment (Figure 5), so that in alkaline media, where the surface charge shows a more negative value, the Si/Ca pigment presents a greater exchange capacity.

FTIR spectra (Figure 6) of the Si/Ca pigment after immersion in 0.5M Na_2SO_4 reveal the appearance of a triplet with an absorption maximum at 616 cm^{-1}, a vibrational band that does not appear in the fresh (unexposed) Si/Ca pigment. At the same time, deformation of the band at 1087 cm^{-1} is observed. These facts suggest modifications in the Si-O-Si bond during immersion. The appearance of the symmetrical absorption band at 616 cm^{-1}, characteristic of

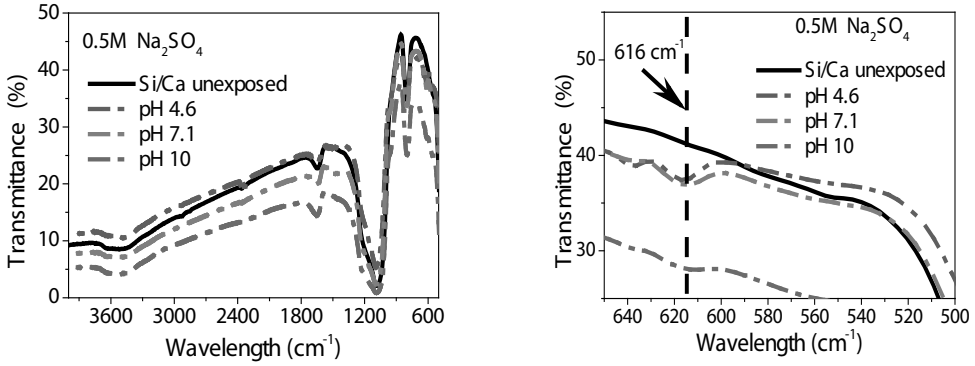

Figure 6. *FTIR spectra of Si/Ca pigment after immersion in 0.5M Na_2SO_4 at different pH values (left) and detail of vibrational band at 616 cm^{-1} (right).*

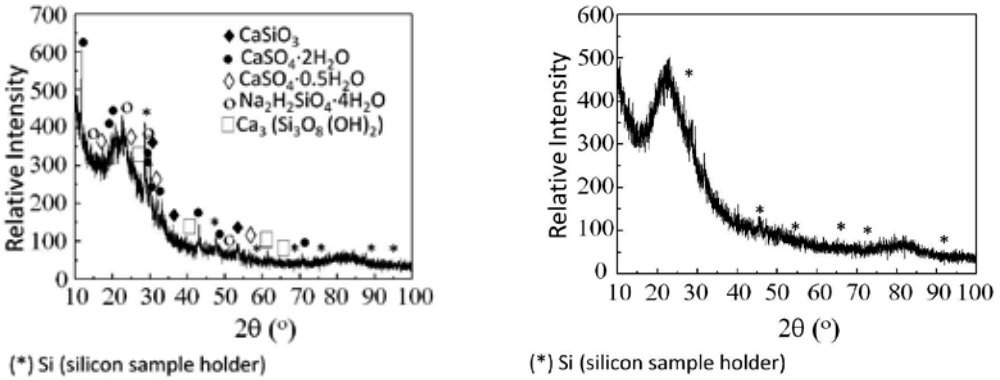

Figure 7 . *X-ray diffractograms of Si/Ca pigment after immersion in 0.5M Na_2SO_4 (left) and in 0.5M NaCl (right) at pH 10.*

In water, the Ca content in solution would be equivalent to the solubility of the pigment, while the calcium content obtained after immersion in 0.5M Na_2SO_4 would represent the result of surface processes, in particular the ion exchange process between the ions of the medium and the Si/Ca. The speciation of calcium detected in the extract on 0.5M Na_2SO_4, of the order of 3.10^{-3} $mol \cdot L^{-1}$ of calcium, indicates that calcium predominates in the form of $CaSO_4$ [15]. Comparison of the inhibiting ion content from the viewpoint of corrosion in the Si/Ca (Ca) and zinc chromate (Cr

the Si-O-Si bond, very typical of silicates and tetrahedral groups $[SiO_4]^{4-}$[27], suggests the transformation of the silanol groups to silicates during immersion of the pigment in 0.5M Na_2SO_4, independently of the medium pH.

The formation of silicates is clearly identified in the XRD study of the pigment exposed in 0.5M Na_2SO_4 solution at pH 10. The X-ray diffractogram (Figure 7, left) shows the appearance of new crystalline phases in the Si/Ca pigment. Peaks appear for wollastonite ($CaSiO_3$) and di- and hemi-hydrated calcium sulphates (gypsum and basanite)

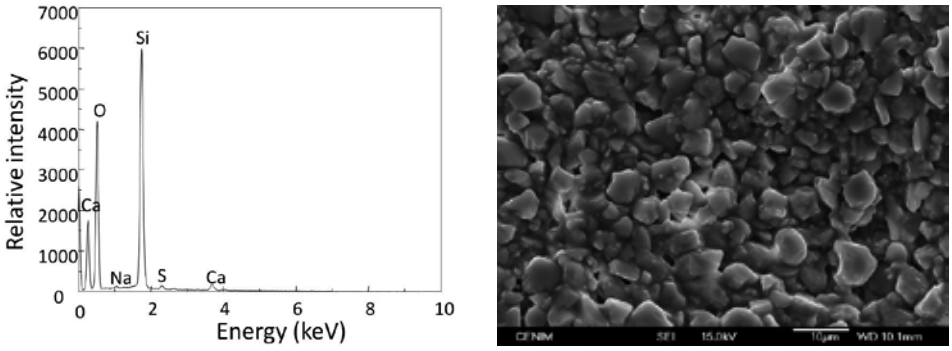

Figure 8. *EDAX spectrum and SEM image of Si/Ca pigment after immersion in 0.5M Na_2SO_4 at pH 10.*

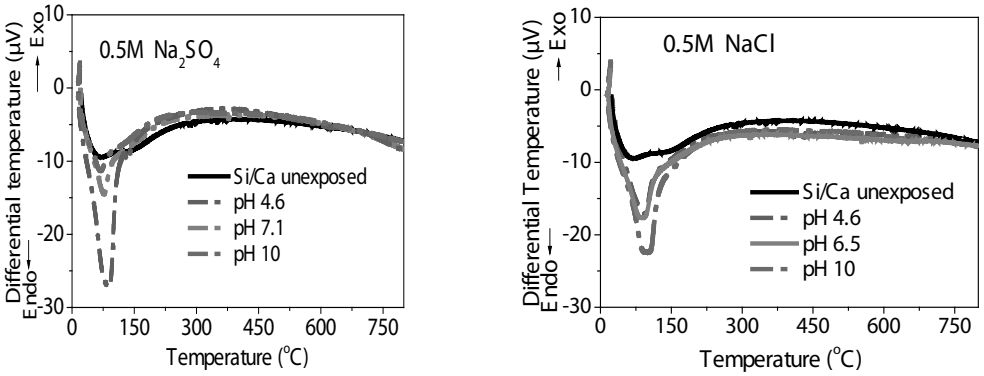

Figure 9. *DTA curves for Si/Ca pigment after immersion in 0.5M Na_2SO_4 (left) and in 0.5M NaCl (right) at different pH values.*

as a consequence of the precipitation of calcium sulphates in the anticorrosive extract. Peaks also appear which may be attributed to a hydrated sodium and hydrogen silicate ($Na_2H_2SiO_4 \times 4H_2O$), formed as a consequence of calcium leaving the solution and the incorporation of hydrogen and sodium cations in the silicate structure, showing the competition between these ions to be incorporated in the network.

The literature contains studies reporting the obtainment of calcium silicates from SiO_2-rich materials (like rice husks) [22,23,28] due to the reactivity of the SiO_2 surface and CaO and/or $Ca(OH)_2$ deposited on the surface of the solid. In many cases the addition of species to the solution [23], to form ionic couples or calcium aquo complexes, assists the controlled precipitation of the silicate, which could be the case in hand, although thermal treatment is the most generalised procedure for forming silicate, since raising the temperature increases the diffusion of calcium towards the interior of the solid, transformations that are observed at 60ºC.

Chemical analysis of the Si/Ca pigment exposed to the 0.5M Na_2SO_4 solution shows a significant rise in the Si/Ca ratio (Table 1). In contrast, the Si/Ca ratio of the pigment exposed in the blank solution is very similar to the initial value and comparable to that of the fresh pigment. The increase in calcium content in the aqueous extract when the pigment is exposed to the sulphate solution indicates a decrease in the calcium content of the solid, and thus an exchange of calcium ions to the aqueous medium, which does not occur with the pigment treated in the blank solution, so these results are indicative of an electrolyte/pigment interaction. Detection of sodium in the pigment and its incorporation in the Si/Ca has been confirmed by XRD, where a sodium and hydrogen silicate phase is observed, pointing to an additional reaction in the ion exchange model traditionally described for the pigment (Figure 1). Finally, an increase in the hydrogen content is seen in the Si/Ca pigment during immersion in 0.5M Na_2SO_4 (table 1), which seems to indicate that the sphere of Si/Ca coordination is affected during immersion of the pigment in the 0.5M Na_2SO_4 solution.

Figure 8 shows the morphology of the pigment after its immersion in 0.5M Na_2SO_4 at pH 10. The particles present an agglomerated and superficially different appearance to the initial solid. This morphological change of the pigment is a consequence of the transformations that take place due to chemical reactions between the pigment and the 0.5M Na_2SO_4 aqueous solution.

Chemical analysis by SEM/EDAX of the pigment obtained after immersion shows variations in the Si/Ca ratio compared to the fresh pigment. Figure 8 depicts the morphology of pigment particles after immersion and a representative EDAX spectrum, in which the Si/Ca ratio is much higher than the initial value of the pigment. In the particles identified in the micrograph, the measured values yield Si/Ca ratios of 15.6 and 29.5. These values indicate a decrease in the calcium content in the pigment after immersion.

Figure 9 (left) shows DTG-TG curves. All the solids exposed in 0.5M Na_2SO_4 show an endothermic peak between 133ºC and 143ºC, corresponding to the loss of water. In the fresh Si/Ca pigment, the endothermic peak occurs at 119ºC. This shift in the dehydration temperature suggests the existence of new hydration compounds in the exposed pigments that were not present in the fresh pigment, corresponding with the drop in the Si/H ratio observed in the composition of the pigment immersed in solution.

Figure 10 shows the variation in mass loss of the pigment exposed in 0.5M Na_2SO_4 at different pH values compared to the fresh pigment. The mass loss remains constant as the pH varies and represents 14.5 wt% of the initial

weight. This value is much higher than the corresponding mass loss of the fresh pigment. Transformation of the Si/Ca pigment during immersion in 0.5M Na_2SO_4 from an amorphous SiO_2 matrix to a more polycrystalline structure, formed of silicates, gypsum and basanite, seems to be related with the observed mass variations.

3.3. Ion exchange capacity of Si/Ca in 0.5M NaCl

The Ca concentration rises in the aqueous extract obtained after immersion of the pigment in 0.5M NaCl solution (Table 2). The exchange capacity of the Si/Ca pigment in NaCl solution is lower than that seen in 0.5M Na_2SO_4 solution throughout the pH range (Figure 5). This figure shows an increase of the exchange capacity as the pH decrease, in contrast to zeta potential measurements, where, as indicated in the ion exchange capacity of Si/Ca in 0.5M Na_2SO_4, the exchange processes are favoured mainly at alkaline pH values. These results may be attributed to a greater dissolution of the Si/Ca pigment in 0.5M NaCl, rather than to a cation exchange itself.

In the FTIR spectra presented in Figure 11 at different pH values, no vibrational band at 616 cm^{-1}, associated with the vibration of tetrahedral $[SiO_4]^{4-}$ groups typical of silicates, is detected, as was the case with the solids exposed in 0.5M Na_2SO_4. Thus, the transformation of silanol groups to silicates observed during immersion of the pigment in 0.5M Na_2SO_4 does not seem to take place during immersion in 0.5M NaCl.

he X-ray diffractogram for Si/Ca exposed in 0.5M NaCl at pH 10 (Figure 7, right) shows the amorphous appearance of the pigment without revealing any new crystalline phases. The appearance of the Si/Ca particles after immersion in 0.5M NaCl at pH 10, obtained by SEM (Figure 12), presents a similar morphology to the initial pigment, corroborating the fact that structural transformations in the Si/Ca have not taken place during immersion in 0.5M NaCl.

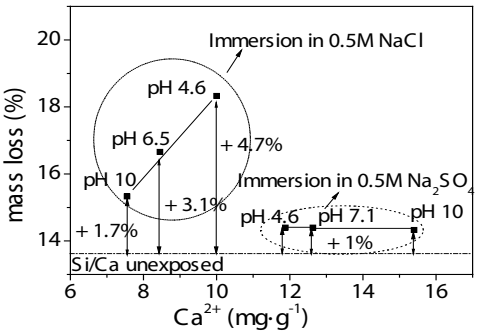

Figure 10. *Relation between mass loss of Si/Ca pigment after immersion in 0.5M Na_2SO_4 and 0.5M NaCl and cation exchange capacity of calcium ions (Ca^{2+}, $mg \cdot g^{-1}$).*

The X-ray diffractogram for Si/Ca exposed in 0.5M NaCl at pH 10 (Figure 7, right) shows the amorphous appearance of the pigment without revealing any new crystalline phases. The appearance of the Si/Ca particles after immersion in 0.5M NaCl at pH 10, obtained by SEM (Figure 12), presents a similar morphology to the initial pigment, corroborating the fact that structural transformations in the Si/Ca have not taken place during immersion in 0.5M NaCl.

DTA-TG curves for the pigment after immersion in 0.5M NaCl solution (Figure 9, right) also show a shift in the endothermic peak corresponding to the dehydration reaction. This modification is coherent with the variation in Si/H ratio values (Table 1), which indicates modifications in the coordination sphere of the pigment as a consequence of immersion in the 0.5M NaCl solution.

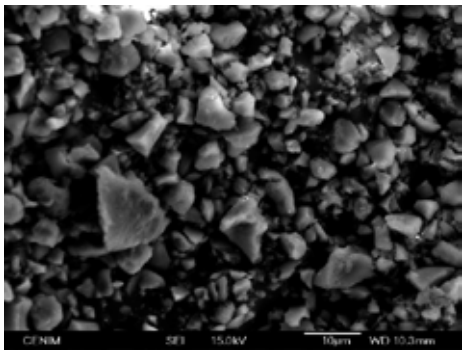

Figure 12. *Morphology of Si/Ca pigment after immersion in 0.5M NaCl at pH 10.*

The mass loss of the Si/Ca pigment exposed in 0.5M NaCl varies between 15.5-18.3 wt% (Figure 10) and is a function of the exchange capacity and thus of the pH of the electrolyte (see Figure 10). The mass loss is greater than that determined for the pigment exposed in the sulphate solution. This mass loss, which is greater for the fresh pigment, is a consequence of the amorphous nature of the pigment after exposure in 0.5M NaCl, in contrast to the Si/Ca exposed in 0.5M Na_2SO_4, which presents a more polycrystalline nature.

4. CONCLUSIONS

A structural transformation of the pigment is deduced from its immersion in 0.5M Na_2SO_4, as detected by FTIR, XRD and SEM. As a consequence of these changes, new phases appear during immersion, mainly silicates ($CaSiO_3$ (wollastonite) and hydrated sodium and hydrogen silicate). The presence of di- and hemi-hydrated calcium sulphates

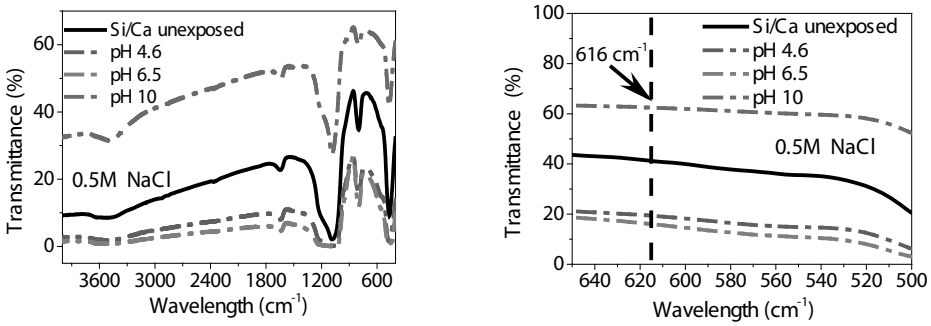

Figure 11. *FTIR spectra of Si/Ca pigment after immersion in 0.5M NaCl at different pH values (left) and detail of vibrational band at 616 cm^{-1} (right).*

indicates possible $CaSO_4$ (co)precipitation processes as a consequence of the speciation of calcium in the solution. The Ca^{2+} ion exchange capacity is greater when the pigment is immersed in 0.5M Na_2SO_4. In this case, calcium ions are exchanged with hydrogen and sodium cations. This exchange is greater at alkaline pH values, in concordance with the observed variation in the zeta potential. In contrast, when the aggressive medium is 0.5M NaCl, a higher calcium content is shown at acid pH values, possibly as a consequence of the greater dissolution of Si/Ca in 0.5M NaCl, rather than to the cation exchange itself.

ACKNOWLEDGEMENTS

This work has been carried out with the financial assistance of the Spanish Ministry of Education and Science to project MAT-2005-06261. The authors are grateful to Grace Davison and Nubiola Inorganic Pigments for supplying the anticorrosive pigments (Shieldex® and zinc chromate) and to Dr. B. Ferrari (ICV- CSIC) for her help in the measures of zeta potential. Dr. N. Granizo, Dr. M. I. Martín and Dr. J. M. Vega express their gratitude to the CSIC of Spain for their contracts through the JAE Programs, co-financed by the European Social Fund.

BIBLIOGRAPHY

1. Langard S, Norseth T (1975) A cohort study of bronchial carcinomas in workers producing chromate pigments. Br J Ind Med 32:62-9
2. Katz SA, Salem H (1993) The toxicology of chromium with respect to its chemical speciation: A review. J Appl Toxicol 13: 217-20.
3. Svoboda M, Mleziva J (1984) Properties of coatings determined by anticorrosive pigments. Prog Org Coat 12(3):251-97
4. Kalendová A (2000) Alkalising and neutralising effects of anticorrosive pigments containing Zn, Mg, Ca, and Sr cations. Prog Org Coat 38:199-06
5. http://www.grace.com.
6. Goldie BPF (1985) Novel Corrosion Inhibitors. Paint Resin 1:16
7. Goldie BPF (1988) Calcium-exchange silica anticorrosion pigment: A reviews. J Oil Col Chem Assoc 71:257-360
8. Zin IM, Bily LM, Gnyp IP, Ratushna MB (2005) Protective action of phosphate and calcium-containing pigments under the conditions of the stress corrosion fracture of steels. Mater Sci 40:605-10
9. Deflorian F, Felhosil S, Rossi L, Fedrizzi P, Bonora L (2002) Performance of primers containing polyphosphate-based ion-exchange pigments for the protection of galvanised steel. Macromol Symp 187:87-96
10. Vasconcelos LW, Margarit ICP, Mattos OR, Fragata FL, Sombra AS (2001) Inhibitory properties of calcium exchanged silica epoxy paintings. Corros Sci 43:2291-03.
11. Armstrong RD, Zhou S (1988) The corrosion inhibition of iron by silicate related materials Corros. Sci 28: 1177-81
12. Amirudin A, Barreau C, Hellouin R, Thierry D (1995) Evaluation of anti-corrosive pigments by pigment extract studies, atmospheric exposure and electrochemical impedance spectroscopy. Prog Org Coat 25:339-55
13. Romagnoli R, Dey MC, Del Amo B (2003)The mechanism of the anticorrosive action of calcium-exchanged silica. Surf Coat Int Part B: Coat Trans 86:135-41
14. Zubielewicz M, Gnot W (2004) Mechanisms of nontoxic anticorrosive pigments in organic waterborne coatings. Prog Org Coat 49:358-71
15. Granizo N. Ph-D Thesis, (2010) Capacidad anticorrosiva de pinturas formuladas con pigmentos de intercambio iónico aplicados sobre acero al carbono, Alcala University, Spain
16. Vega JM. Ph-D Thesis, (2011) Mecanismos de protección anticorrosiva del aluminio mediante recubrimientos de pintura formulados con pigmentos de intercambio iónico, Complutense University, Spain
17. Chico B, Simancas J, Vega JM, Granizo N, Diaz I, de la Fuente D, Morcillo M (2008) Anticorrosive behaviour of alkyd paints formulated with ion-exchange pigments. Prog Org Coat 61:283-90
18. Araujo-Andrade C, Ortega-Zarzosa G, Ponce-Castañeda S, Martínez JR (2000) Análisis de las reacciones de hidrólisis y condensación en muestras de sílica xerogeles usando la espectroscopia infrarroja. Rev Mex Fis 46:593-97
19. Martínez JR, Ruiz R (2002) Mapeo estructural de sílica xerogel utilizando la espectroscopía infrarroja. Rev Mex Fis 48:142-9
20. Martínez JR, Ruiz F, De la Cruz-Mendoza JA, Villaseñor-González P (1990) Formación y caracterización de materiales vítreos preparados por la técnica sol-gel. Rev Mex Fis 45:472-9
21. Serrano SS, Prieto-García F, Gordillo-Martínez AJ (2005) Síntesis y caracterización de Sílice dopada con óxidos de hierro por la vía Sol-Gel. Rev Latin Am Metal Mater 25:3-14
22. Ahumada LM, Rodríguez-Páez JE (2006) Uso del SiO2 obtenido de la cascarilla de arroz en la síntesis de silicatos de calcio. Rev Acad Colomb Cien Exact Fís Nat 30:581-94
23. Rodríguez-Páez JE, Ahumada LM, Bustamante JM, Ruiz de Murgueitio J (2005) Obtención de silicatos de calcio utilizando el método de precipitación controlada. Bol Sol Esp Ceram V 44:421-6
24. Carta D, Knowles JA, Smith ME. Newport RJ (2007) Synthesis and structural characterization of P2O5–CaO–Na2O sol–gel materials. J Non-Cryst Solids 353:1141-9
25. Chen SK, Liu HS (1994) FTIR, DTA and XRD study of sphene (CaTiSiOs) crystallization in a ceramic frit and a non-borate base glass. J Mater Sci 29:2921-30
26. Handke M, Mozgawa W (1995) Model quasi-molecule Si2O as an approach in the IR spectra description glassy and crystalline framework silicates. J Mol Struct 548;341-4
27. Gorman-Lewis D, Skanthakumar S, Jensen MP, Mekki S, Nagy KL, Soderholm L (2008) FTIR characterization of amorphous uranyl-silicates. Chem Geol 253:136-40
28. Treviño B, Gómez I (2002) Obtención de fases del cemento utilizando desechos agrícolas e industriales. Ciencia UANL. University Autónoma of Nuevo León 2:19-196-01